Intensity dependence of the photoreflectance amplitude in semiconductors

Robert E. Wagner and Andreas Mandelis
Photothermal and Optoelectronic Diagnostics Laboratory, Department of Mechanical Engineering, University of Toronto, Toronto, Canada M5S 1A4
(Received 23 February 1994; revised manuscript received 22 July 1994)

A rigorous calculation of the intensity dependence of the photoreflectance (PR) amplitude is presented, and the derived relation is compared with published experimental results. The method utilizes a Taylor-series expansion to determine the change in reflectance in terms of the modulation of the surface electric field, and the Fourier-series technique is employed to explicitly develop the harmonic components of the photoreflectance amplitude for square-wave excitation. In particular, it is shown that if the photoreflectance amplitude depends upon the optical excitation intensity I as $\ln(\gamma I+1)$, which is normally the case experimentally, then the small-modulation PR signal should have a line shape proportional to the first derivative of the sample reflectance with respect to the surface electric field. In the high-field limit, the nature of the Franz-Keldysh oscillations is explained for both small- and large-modulation conditions, and the theoretical predictions are correlated with recent experimental data. Overall, this theoretical study of the photoreflectance effect clarifies certain issues regarding the connection between the observed intensity dependence of the PR amplitude and the PR line shape, and it also illustrates how the nature of the PR line shape changes as one moves from low- to high-field conditions, in both the small- and large-modulation limits.

I. INTRODUCTION

In recent years, the photoreflectance (PR) effect has been used quite extensively to probe the optical and electronic properties of semiconductors.[1,2] The basic configuration used for measuring the PR signal is as follows. A semiconductor sample is illuminated with a beam of super-band-gap photons (usually monochromatic) which is chopped (modulated) at a frequency f; the intensity of this pump beam is usually in the range $0.01-100$ mW/cm^2. The pump beam creates a modulation in the sample reflectance which is monitored via a second unmodulated optical beam, the probe beam, which is usually obtained from a lamp source. Phenomenologically, a small fraction of the reflected probe beam is modulated as a result of its interaction with the optically excited sample. The PR signal is strongly dependent on the probe wavelength; therefore, the optical system for the probe beam often contains a monochromator, making the probe tunable over a significant wavelength range.

In physical terms, for a homogeneous sample, the mechanism responsible for the modulation of the reflectance by the pump beam is as follows.[1] When super-band-gap pump photons are absorbed by the sample, they excite electrons from the valence band to the conduction band. Due to the built-in electric field which normally exists within the sample, the nonequilibrium free carriers are spatially separated: For an n-type material, if the surface built-in field is associated with a depletion layer, free electrons drift into the bulk, and holes collect at the surface; on the other hand, if the surface field is due to an accumulation layer, free electrons drift towards the surface, and holes into the bulk. For a p-type material, if the surface built-in field is associated with a depletion layer, holes drift into the bulk, and free electrons collect at the surface; alternatively, if the surface field is due to an accumulation layer, holes drift towards the surface, and free electrons into the bulk. Overall, the electrons and holes are separated by the built-in field, and an opposing photo field is generated which decreases the magnitude of the built-in field; therefore, the magnitude of the surface field is modulated by the pump beam. Since the optical properties of a semiconductor are known to be a function of the electric field within the sample (the Franz-Keldysh effect), especially near sample critical points, photomodulation of the built-in field will cause the reflectance of the sample to be modulated; this is known as the photoreflectance effect.

It should be noted that the dependence of the PR signal upon the modulation frequency is, among other things, a function of the surface-state density, and the ability of the surface states to capture minority and/or majority carriers. Shen *et al.*[3] have clearly described the dynamics of the photoreflectance effect in undoped GaAs. They point out that when the excitation beam is on, one must consider the interaction of the surface traps with both the minority and majority carriers, and when the excitation beam is off, the interaction of the surface traps with the majority carriers.

For example, consider the situation of a depletion layer at the surface of an n-type material, with a large density of electrons in surface states which can easily capture minority hole carriers.[3] Therefore, when photogenerated holes drift to the sample surface during a PR experiment, the holes are captured efficiently by the surface-state electrons, resulting in a localized positive charge at the surface. When the optical excitation beam is turned off, the built-in field will not relax to its dark value until the positively charged surface states capture excess electrons from the conduction band; this process will occur within

the period of time τ_{ss}, which is the electron-trapping time.[4] Overall, when surface trapping is significant, the PR signal should be independent of frequency until $\omega\tau_{ss} > 1$; then, at higher frequencies, the PR amplitude will begin to decline.

In the absence of surface trapping, one would expect the relaxation of the surface field to its dark value to depend upon the bulk recombination time of the carriers; in this case, the PR signal would be essentially independent of modulation frequency until $\omega\tau > 1$, where τ is the band-to-band recombination lifetime of the free carriers.

Various groups have used the frequency response of the PR amplitude to obtain the surface-state relaxation time.[4–7] The trapping times obtained at room temperature are on the order of 1 ms for Si and GaAs. There appear to be no reported PR experiments which show a frequency response sensitive to the bulk recombination time.

Taking into account the PR signal generation mechanism described above, the question of the PR magnitude variation with the intensity of the pump beam arises. In addressing this question, an expression for the PR amplitude as a function of the pump-beam intensity will be developed. The following theoretical treatment is applicable to both the creation of a small perturbation in the built-in electric field, as well as for strong perturbations, in which case it will be shown that a substantially different PR line shape is obtained. The above-mentioned calculation was deemed to be important because, as will be shown later, the experimental intensity dependence of the PR amplitude has been found to have a variety of functional dependences, including logarithmic and various sublinear power laws. Also, there has been no clear description of how the PR line shape should vary as the equilibrium built-in field is increased from zero, and how the line shape should change when the small-modulation to large-modulation transition is made.

In 1990, Kanata *et al.*[8] presented a theoretical model which accounted for the intensity dependence of the PR effect. The main aim of their work was to determine the dependence of the PR amplitude upon the surface voltage of the semiconductor sample, and hence, to show that the PR amplitude can be used to probe the surface voltage. By measuring the temperature dependence of the PR signal for a number of samples, they determine the surface voltage via an Arrenhius-type analysis. Although the work of Kanata *et al.* is informative, it neglects certain aspects of the PR problem. For example, the explicit determination of the various harmonic components of the signal was not performed for the assumed square-wave excitation. More importantly, in the small-modulation limit, a Taylor-series expansion was not employed, so the nature of the PR line shape is not apparent. Therefore, another theoretical analysis of the PR intensity dependence will be presented, and a number of interesting observations will be made.

II. THEORY AND DISCUSSION

Consider that at equilibrium the built-in field of a semiconductor is confined to a layer of finite thickness at the sample surface, the space-charge layer (SCL). For *n*-type materials, the SCL is termed a depletion layer when it is positively charged, and an accumulation layer when it is negatively charged; for a *p*-type material the SCL is termed a depletion layer when it is negatively charged, and an accumulation layer when it is positively charged. The electric-field distribution in the SCL can be obtained by solving the one-dimensional Poisson equation:

$$\frac{d^2V(x)}{dx^2} = -\frac{\rho(x)}{\epsilon_{dc}\epsilon_0} , \tag{1}$$

where $V(x)$ is the potential, $\rho(x)$ is the net charge density, x is the distance into the sample from the surface, ϵ_{dc} is the low-frequency dielectric constant (real), and ϵ_0 is the permittivity of free space.

Assuming that ρ is constant in the SCL, Eq. (1) can be integrated once to yield

$$\frac{dV(x)}{dx} = -\frac{\rho}{\epsilon_{dc}\epsilon_0}x + C_1 , \tag{2}$$

where C_1 is a constant. Since the SCL has a finite thickness of W in the abrupt approximation, the electric field must be zero at $x = W$. Thus, $dV/dx = 0$ at $x = W$. Applying this condition to Eq. (2) gives

$$\frac{dV}{dx} = \frac{\rho}{\epsilon_{dc}\epsilon_0}(W - x) . \tag{3}$$

Next, integrating Eq. (3) yields

$$V(x) = -\frac{\rho}{2\epsilon_{dc}\epsilon_0}(x - W)^2 \tag{4}$$

when it is assumed that $V(W) = 0$. The voltage at the surface can be found by letting $x = 0$ in Eq. (4).

$$V_S = -\frac{\rho W^2}{2\epsilon_{dc}\epsilon_0} , \tag{5}$$

and then W can be expressed in terms of V_S,

$$W = (2\epsilon_{dc}\epsilon_0)^{1/2}\left[-\frac{V_S}{\rho}\right]^{1/2} . \tag{6}$$

Equation (6) is expressed explicitly in terms of $-V_S/\rho$ because this quantity is always positive; from Eq. (5), $-V_S/\rho$ is equal to a positive constant times W^2, which is positive.

Finally, the electric field $\xi(x)$ can be determined from Eq. (3),

$$\xi(x) = -\frac{dV(x)}{dx} = \frac{\rho}{\epsilon_{dc}\epsilon_0}(x - W) , \tag{7}$$

and the surface value of the field is

$$\xi_S = -\frac{\rho W}{\epsilon_{dc}\epsilon_0} . \tag{8}$$

Next, assume that when the probe beam is reflecting from the sample surface, it does not penetrate into the bulk; therefore, the sample reflectance R only depends upon the value of the built-in electric field at the surface, ξ_S. If this is not the case, then the field modulation must be averaged over the penetration depth of the probe beam

(see Appendix A). Taking into account that $R=R(\xi_S)$, an expression for the photoreflectance component of the reflectance modulation can be written as

$$\Delta R_{\mathrm{PR}}=\frac{\partial R}{\partial \xi_S}\Delta\xi_S+\cdots+\frac{1}{n!}\frac{\partial^n R}{\partial \xi_S^n}(\Delta\xi_S)^n+\cdots , \quad (9)$$

where Eq. (9) is the Taylor-series expansion for ΔR_{PR}. If it is assumed that the modulated surface field has as its minimum the dark value, then

$$\Delta\xi_S=\xi_{S,1}-\xi_{S,0} , \quad (10)$$

where $\xi_{S,1}$ is the surface field under illumination, and $\xi_{S,0}$ is the surface field in the dark. All of the derivatives in Eq. (9) are evaluated using the dark value of the surface field. In general, the derivatives of Eq. (9) are not easy to calculate, and they depend strongly on the model used to describe the optical properties of the sample. The derivation of a relation for $\Delta\xi_S$ is somewhat easier. First, it is convenient to express ξ_S in terms of V_S; using Eqs. (5) and (8):

$$\xi_S=C_2\left[\frac{-V_S}{\rho}\right]^{1/2} , \quad (11)$$

where

$$C_2\equiv-\rho\left[\frac{2}{\epsilon_{\mathrm{dc}}\epsilon_0}\right]^{1/2} . \quad (12)$$

Furthermore, an expression for the surface voltage in the presence of N photogenerated carriers is readily available:[6]

$$V_S=V_{S,O}\pm\frac{k_BT}{e}\ln(bN+1) , \quad (13)$$

where $V_{S,O}$ is the equilibrium surface voltage, k_B is the Boltzmann constant, T is the absolute temperature, e is the electronic charge, b is a constant, and N is the photogenerated free-carrier density. For an n-type material, the $+$ ($-$) sign applies to a depletion (accumulation) layer, and the opposite is true for a p-type material. Next, substituting Eq. (13) into (11) yields

$$\xi_{S,1}=C_2\left[\frac{-V_{S,0}}{\rho}\mp\frac{k_BT}{e\rho}\ln(bN+1)\right]^{1/2} . \quad (14)$$

Under small-modulation excitation conditions,

$$|V_{S,0}|\gg\frac{k_BT}{e}\ln(bN+1) . \quad (15)$$

Therefore,

$$\xi_{S,1}\approx\xi_{S,0}\left[1\pm\frac{k_BT}{2eV_{S,0}}\ln(bN+1)\right] . \quad (16)$$

Furthermore, if

$$C_3\equiv\pm\frac{k_BT}{2eV_{S,0}}\xi_{S,0} , \quad (17)$$

then

$$\xi_{S,1}\approx\xi_{S,0}+C_3\ln(bN+1) . \quad (18)$$

Finally, using Eq. (10)

$$\Delta\xi_S\approx C_3\ln(bN+1) . \quad (19)$$

Next, it will be assumed that the sample is excited with an optical beam for which the intensity is modulated in a square-wave manner between 0 and I, at the angular frequency ω. Also, it will be assumed that the frequency is low, so that the period of the exciting beam ($2\pi/\omega$) is much longer than the relaxation time of the photovoltage; thus, when the light is on, $\Delta\xi_S$ achieves the value $C_3\ln(bN+1)$, and when the light is off, $\Delta\xi_S$ goes to zero. In addition, under low-level modulation conditions it is likely that N is a linear function of I, so

$$\Delta\xi_S\approx C_3\ln(\gamma I+1) , \quad (20)$$

where γ is a constant which is proportional to b. Taking into account the above conditions, the time history of $\Delta\xi_S$ is the simple square wave depicted in Fig. 1.

$\Delta\xi_S(t)$ can be written as

$$\Delta\xi_S(t)\approx C_3\ln(\gamma I+1)f(t) , \quad (21)$$

where $f(t)$ is a square-wave modulation function with a range (0,1). When Eq. (21) is substituted into Eq. (9), the result is

$$\Delta R_{\mathrm{PR}}(t)=f(t)\left\{\frac{\partial R}{\partial\xi_S}C_3\ln(\gamma I+1)+\cdots+\frac{1}{n!}\frac{\partial^n R}{\partial\xi_S^n}[C_3\ln(\gamma I+1)]^n+\cdots\right\} . \quad (22)$$

From Eq. (22) it should be clear that for square-wave modulation, the PR line shape is completely determined by the terms within the curly brackets; thus, all harmonics of the PR signal should yield the same line shape.

The function $f(t)$ of Eq. (22) will now be expressed as a Fourier series, so that the various harmonic components of $\Delta R_{\mathrm{PR}}(t)$ can be rigorously obtained:

$$f(t)=\frac{a_0}{2}+\sum_{k=1}^{\infty}a_k\cos(k\omega t)+\sum_{k=1}^{\infty}b_k\sin(k\omega t) , \quad (23)$$

where

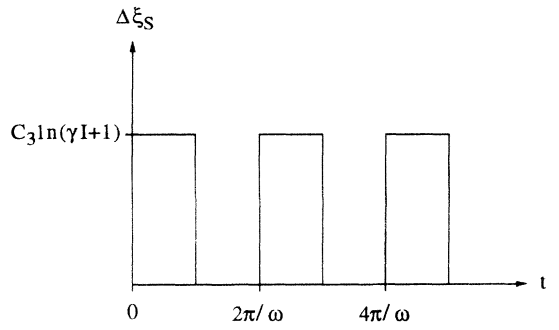

FIG. 1. Time history of $\Delta\xi_S$ for square-wave excitation.

$$a_k=\frac{\omega}{\pi}\int_0^{2\pi/\omega}f(t)\cos(k\omega t)dt\ , \tag{24}$$

and

$$b_k=\frac{\omega}{\pi}\int_0^{2\pi/\omega}f(t)\sin(k\omega t)dt\ . \tag{25}$$

When Eq. (23) is evaluated up to the fifth harmonic, the result is

$$f(t)=\tfrac{1}{2}+\frac{2}{\pi}[\sin(\omega t)+\tfrac{1}{3}\sin(3\omega t)+\tfrac{1}{5}\sin(5\omega t)+\cdots]\ . \tag{26}$$

Clearly, the magnitude of the nth harmonic tends to decrease as n increases. Overall, all of the information contained in the PR signal can be obtained by measuring the first-harmonic component of the signal.

From Eqs. (22) and (26), the magnitude of the first harmonic of the PR signal is

$$\Delta R_{\mathrm{PR},\omega}=\frac{2}{\pi}\left[\sum_{n=1}^{\infty}\frac{[C_3\ln(\gamma I+1)]^n}{n!}\frac{\partial^n R}{\partial\xi_S^n}\right]\ . \tag{27}$$

Note that when $n=1$, the following term is obtained:

$$\Delta R_{\mathrm{PR},\omega}(n=1)=\frac{2}{\pi}C_3\ln(\gamma I+1)\left[\frac{\partial R}{\partial\xi_S}\right]\ . \tag{28}$$

This term provides a PR signal component which is proportional to the natural logarithm of the excitation intensity when $\gamma I\gg 1$, which is normally the case.

The type of intensity dependence indicated by Eq. (28), $\Delta R\propto\ln(\gamma I+1)$, with $\gamma I\gg 1$, has been observed by several groups during PR measurements on homogeneous semiconductors. For example, Stossel, Colbow, and Dunn[9] found a $\ln(I)$ dependence during PR measurements on CdS. Also, Shen *et al.*[6] observed a $\ln(I)$ dependence over three orders of magnitude during PR measurements on Si.

On the other hand, several other reports dealing with the PR effect concluded that the PR amplitude was proportional to the laser pump intensity to the $\frac{1}{3}$ power, for example, Shay,[10] Nahory and Shay,[11] and Broser, Hoffmann, and Schulz.[12] It is interesting to note that the functions $\ln(x)$ and $x^{1/3}$ increase in a similar manner over the range $15\le x\le 200$ [Fig. 2(a)]; therefore, it is possible that these groups were actually observing a PR intensity dependence of the form $\Delta R\propto\ln(I)$.

Finally, Bauer *et al.*[13] observed an intensity dependence of the form $x^{1/2}$ over a limited range of pump power, with the PR signal appearing to saturate at higher intensities. It is interesting to note that the functions $\ln(x)$ and $x^{1/2}$ increase in a similar manner over the range $4\le x\le 20$ [Fig. 2(b)], and that the $\ln(x)$ function decreases more slowly with x for $x>20$. In fact, the $\ln(x)$ function can be fitted very well to the date presented by Bauer *et al.* over the entire measurement range of two orders of magnitude, while the $x^{1/2}$ function only matches the data over half the intensity range. Therefore, it appears that the PR vs intensity data of Bauer *et al.*, are better described by the $\ln(x)$ function than by the $x^{1/2}$ function, consistent with the present theoretical considerations.

Judging from the selection of experimental data discussed above, the intensity dependence of the PR amplitude is best described by a function of the form $\ln(\gamma I+1)$, or $\ln(I)$ when $\gamma I\gg 1$. Thus, in the small-modulation limit, it appears that the line shape of a PR spectrum is usually determined by the first derivative of R with respect to the surface electric field [Eq. (28)]. Since no experimental PR data have been obtained which show an intensity dependence of the form $[\ln(\gamma I+1)]^n$ $(n>1)$, it can be concluded that the $n>1$ terms of Eq. (27) do not contribute to the PR line shape. There are two possible reasons why the $n>1$ terms are not significant: First, the partial derivatives of Eq. (27) may decrease dramatically in magnitude for $n>1$; and second, the factor $[C_3\ln(\gamma I+1)]^n/n!$ may decrease quickly for $n>1$. Note that the line shapes expected from the $n>1$ partial derivatives of Eq. (27) are calculated in Appendix B.

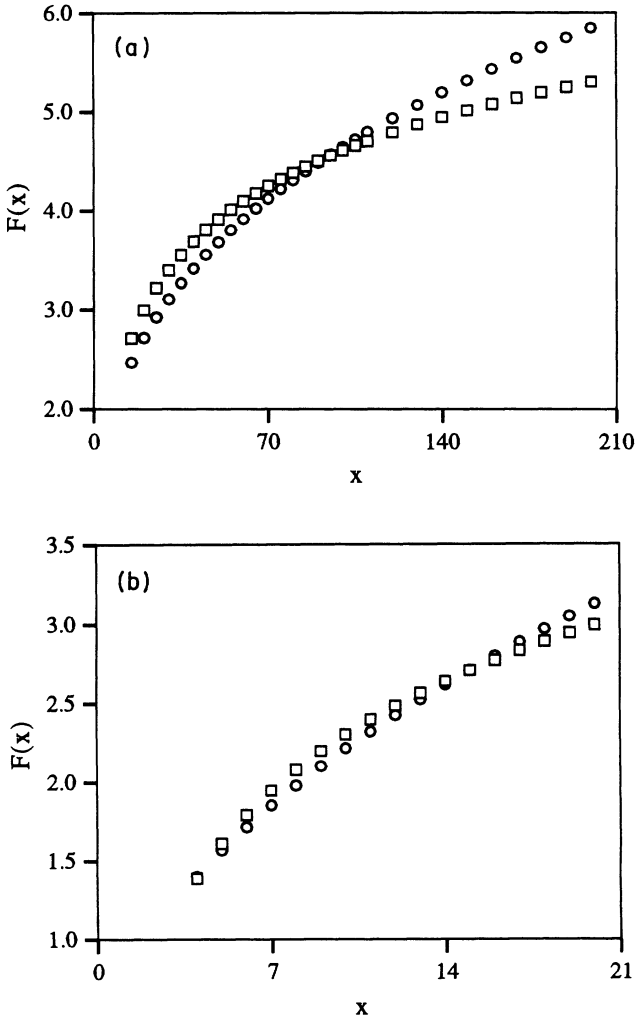

FIG. 2. (a) Comparison of the functions $F(x)=\ln x$ (□) and $F(x)=x^{1/3}$ (○), over the range $15\le x\le 200$. (b) Comparison of the functions $F(x)=\ln(x)$ (□) and $F(x)=0.7x^{1/2}$ (○), over the range $4\le x\le 20$.

The nature of $\partial R/\partial\xi_S$ will now be considered. In the previously identified, zero-optical-penetration limit, the following expression can be written for $R(\xi_S)$:[14]

$$R(\xi_S)=R_0\{1+\mathrm{Re}[(\alpha-i\beta)\Delta\epsilon(\xi_S)]\}\ , \tag{29}$$

where R_0 is the zero-field reflectance, Re denotes "the real part of," $\Delta\epsilon$ is the change in the dielectric constant induced by the electric field, and α,β are the Seraphin coefficients;[15]

$$\alpha=2d_1/(d_1^2+d_2^2)\ , \tag{30}$$

$$\beta=2d_2/(d_1^2+d_2^2)\ , \tag{31}$$

where

$$d_1=\frac{n}{n_0}(n^2-3k^2-n_0)\ , \tag{32}$$

$$d_2=\frac{k}{n_0}(3n^2-k^2-n_0)\ . \tag{33}$$

Here n and k are the refractive index and extinction coefficient, respectively, of the sample under no-field conditions, and n_0 is the refractive index of the nonabsorbing medium of incidence (e.g., air or vacuum). Differentiating Eq. (29) once, the following expression is obtained:

$$\frac{\partial R}{\partial\xi_S}=R_0\mathrm{Re}\left[(\alpha-i\beta)\frac{\partial(\Delta\epsilon)}{\partial\xi_S}\right]\ . \tag{34}$$

The actual form of $\Delta\epsilon$ depends upon the type of model used to describe the optical properties of the sample. For a single electron in a periodic potential, and neglecting Coulomb effects (electron-electron interactions), $\Delta\epsilon$ can be written[14]

$$\Delta\epsilon(\xi_S)_{\mathrm{lf}}\propto\xi_S^2\frac{1}{E^2}\frac{\partial^3}{\partial E^3}[E^2\epsilon(E)]\ , \tag{35}$$

when the "low-field" limit is valid. E is the probe photon energy. The low-field limit only applies when the surface electric field has a magnitude less than about 10^3 V/cm.[16] Unfortunately, the equilibrium built-in electric field at the surface of a typical semiconductor is more likely to be around 10^5 V/cm.[17] Therefore, a high-field relation must often be used in place of Eq. (35).

Under certain conditions the low-field approximation may indeed be valid; in this case, using Eq. (34) one obtains

$$\frac{\partial R}{\partial\xi_S}\propto\frac{\xi_{S,0}R_0}{E^2}\mathrm{Re}\left\{(\alpha-i\beta)\frac{\partial^3}{\partial E^3}[E^2\epsilon(E)]\right\}\ . \tag{36}$$

When Eq. (36) is substituted into (28), ΔR is found to give the traditional third-derivative line shape[14] (i.e., the third derivative of ϵ with respect to E, the probe photon energy). It is also interesting to note that in the low-field limit, ΔR_{PR} appears to be independent of the equilibrium surface field. This is not really the case, since the constant b in Eq. (13) is actually a function of $V_{S,0}$: As $V_{S,0}$ is increased from zero, b also increases from zero. In other words, as $V_{S,0}$ is increased, the photovoltage becomes larger for a given value of N.

Instead of using a low-field expression for $\Delta\epsilon$, a high-field relation should often be employed; for instance, again ignoring Coulomb effects one may write[14]

$$\Delta\epsilon(\xi_S)\propto\frac{1}{E^2}\xi_S^{1/3}[G(z)+iF(z)]\ , \tag{37}$$

where

$$z=p(E)\xi_S^{-2/3} \tag{38}$$

and

$$p(E)\equiv(E_g-E)\left[\frac{8\pi^2\mu}{e^2h^2}\right]^{1/3}\ , \tag{39}$$

where E_g is the energy gap of the semiconductor, μ is the interband effective mass, and h is Planck's constant. Note that the expressions used in this paper are for an M_0 critical point (such as the direct fundamental gap), and that broadening has been ignored. Expressions similar to Eqs. (37)–(39) are available for other types of critical points, and have been given by Aspnes.[18]

With regard to $G(z)$ and $F(z)$, these are given by Aspnes:[14]

$$F(z)=\pi[\mathrm{Ai}'^2(z)-z\,\mathrm{Ai}^2(z)]-(-z)^{1/2}u(-z) \tag{40}$$

and

$$G(z)=\pi[\mathrm{Ai}'(z)\mathrm{Bi}'(z)-z\,\mathrm{Ai}(z)\mathrm{Bi}(z)]+z^{1/2}u(z)\ , \tag{41}$$

where Ai and Bi are Airy functions,[19] the prime denotes a derivative with respect to z, and $u(z)$ is the unit step function [i.e., $u(-z)$ is zero when $z>0$, and $u(z)$ is zero when $z<0$; otherwise, u is 1]. At this point we can write

$$\frac{\partial(\Delta\epsilon)}{\partial\xi_S}\propto E^{-2}[\tfrac{1}{3}\xi_S^{-2/3}(G+iF)-\tfrac{2}{3}p\xi_S^{-4/3}(G'+iF')]\ , \tag{42}$$

where the primes indicate derivatives with respect to z. Making use of Eqs. (40) and (41), and the differential equation for the Airy functions:

$$w(z)''-zw(z)=0\ , \tag{43}$$

it is easy to show that the range $-\infty<z<\infty$:

$$F'=-\pi\,\mathrm{Ai}^2(z)+\tfrac{1}{2}(-z)^{-1/2}u(-z)\ , \tag{44}$$

$$G'=-\pi\,\mathrm{Ai}(z)\mathrm{Bi}(z)+\tfrac{1}{2}z^{-1/2}u(z)\ . \tag{45}$$

Finally, Eq. (42) can be evaluated using the series solutions for Ai(z) and Bi(z), and their derivatives. For instance, in the range $-3.2<z<3.2$, Ai(z), Ai'(z), Bi(z), and Bi'(z) can be calculated using relations 10.4.2 to 10.4.5 given by Antosiewicz.[19] Also, in the range $z<-3.2$, relations 10.4.69, 10.4.70, and 10.4.78–10.4.81 can be used to evaluate the various Airy functions.[19]

Using the methodology described above, it is possible to determine the PR line shape in the high-field limit. In order to probe the change in line shape as the field is increased, a simulation will be carried out for the PR signal in the vicinity of the fundamental absorption edge for GaAs, a direct-gap semiconductor.

Utilizing the theoretical relations given by Aspnes and

Bottka,[20] it can be shown that for a direct-gap semiconductor, the conduction-band–valence-band contribution to the dielectric constant is

$$\epsilon_1(E \geq E_g) = \phi + \frac{A}{E^2}[2E_g^{1/2} - (E_g + E)^{1/2}] , \quad (46)$$

$$\epsilon_1(E < E_g) = \phi + \frac{A}{E^2}[2E_g^{1/2} - (E_g - E)^{1/2} - (E_g + E)^{1/2}] , \quad (47)$$

and

$$\epsilon_2(E \geq E_g) = \frac{A}{E^2}(E - E_g)^{1/2} , \quad (48)$$

where A is a positive constant, and ϕ has a theoretical value of one. Kudman and Seidel[21] have measured the absorption coefficient for GaAs in the vicinity of E_g (1.39 eV); they found that

$$\epsilon_2(E \geq E_g) = 2.6 \times 10^{-28} \frac{(E - E_g)^{1/2}}{E^2} , \quad (49)$$

where the numerical prefactor is the quantity $A[J^{3/2}]$, and E, E_g have units of $[J]$. Although the value of A in Eq. (49) yields an accurate value for ϵ_2 in the range $1.4 < E < 1.7$ eV, when the same value of A is used to determine ϵ_1 via Eqs. (46) and (47), ϵ_1 is grossly underestimated. This is not surprising since Eqs. (46) and (47) are based on a relation for ϵ_2 which is only accurate near E_g. Therefore, the theoretical relations for ϵ_1 will be made more realistic by letting the constant ϕ in Eqs. (46) and (47) be equal to 12.

When the low-field approximation is valid, Eqs. (46)–(48) can be used to evaluate Eq. (36); when $E \geq E_g$,

$$\frac{\partial R}{\partial \xi_S} \propto \frac{-R_0 \xi_{S,0}}{E^2}[\alpha(E_g + E)^{-5/2} - \beta(E - E_g)^{-5/2}] . \quad (50)$$

Likewise, when $E < E_g$,

$$\frac{\partial R}{\partial \xi_S} \propto \frac{-R_0 \xi_{S,0}}{E^2}\alpha[(E_g + E)^{-5/2} - (E_g - E)^{-5/2}] . \quad (51)$$

In fact, the unbroadened line shapes given by Eqs. (50) and (51) are far sharper than found experimentally; therefore, the PR line shape is usually found by using a relation for ϵ which includes broadening through the phenomenological parameter Γ:[16]

$$\epsilon(E) \propto E^{-2}(E - E_g + i\Gamma)^{1/2} . \quad (52)$$

In the classical framework of the optical absorption model, Γ is related to the damped harmonic oscillator. Substituting Eq. (52) into (36) yields the broadened, low-field line shape function:

$$\frac{\partial R}{\partial \xi_S} \propto \frac{R_0 \xi_{S,0}}{E^2}\mathrm{Re}[(\alpha - i\beta)(E - E_g + i\Gamma)^{-5/2}] . \quad (53)$$

Equation (53) is plotted in Fig. 3 for $\Gamma = 10$ meV; the sample is assumed to be GaAs with $E_g = 1.39$ eV, and (α, β) are calculated via Eqs. (46)–(48).

If the Franz-Keldysh theory is used to determine the high-field PR line shape, the result is quite different from that shown in Fig. 3. For instance, Fig. 4 shows the GaAs PR line shape assuming that μ is 0.1 times the free-electron mass; the equilibrium surface field is 5×10^7 V/m; and the modulation of the surface field is small relative to its equilibrium magnitude, in which case Eq. (42) gives the PR line shape. With regard to the nature of the high-field line shape of Fig. 4, it should be apparent that the PR spectrum displays the characteristic Franz-Keldysh oscillations, and that the amplitude of the envelope does not decay as E becomes much greater than E_g; such behavior has been observed experimentally by Bhattacharya *et al.*[2] Note that Cardona, Shaklee, and Pollak[22] have considered a related type of behavior, albeit to a lesser extent, for electroreflectance experiments.

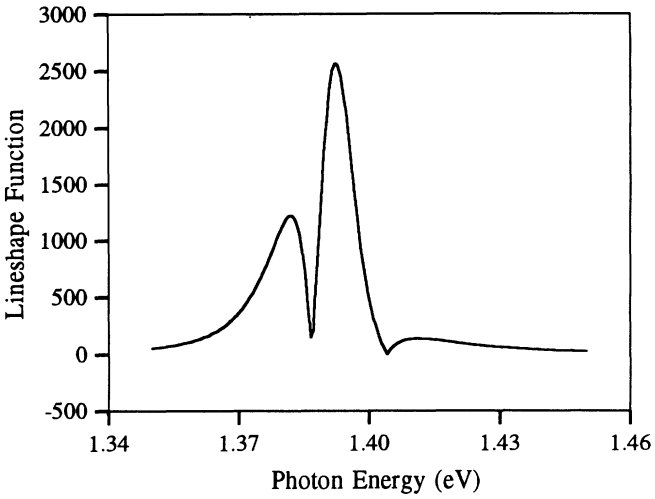

FIG. 3. The low-field PR line-shape function [Eq. (53)] vs the photon energy, in the vicinity of the GaAs direct energy gap (1.39 eV). The broadening parameter Γ is 10 meV.

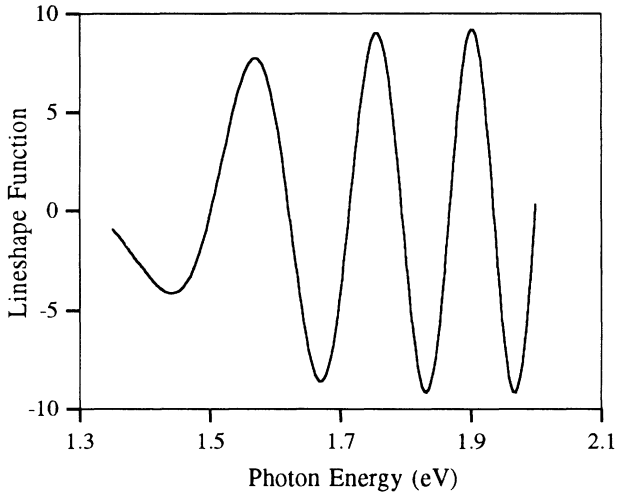

FIG. 4. The high-field, small-modulation PR line-shape function [Eq. (42)] vs the photon energy, in the vicinity of the GaAs direct energy gap (1.39 eV). The effective mass is 0.1 times the free electron mass, and $\xi_{S,0} = 5 \times 10^7$ V/m.

With regard to the results of Bhattacharya *et al.*[2], they obtained PR and electroreflectance (ER) data for an InP Schottky barrier. Of further interest, they found that the nature of the PR Franz-Keldysh (FK) oscillations changed when the magnitude of the surface field was increased. In particular, the FK oscillations were not damped significantly when the surface field was largest (bias >9 V), which corresponds with the behavior depicted in Fig. 4. On the other hand, when the surface field was lower (bias <1.5 V), the FK oscillations were damped heavily as the probe photon energy was increased. This type of damped behavior cannot be obtained if one assumes that the optical beam is only perturbing the sample electric field by a small amount; in fact, heavily damped FK oscillations can only be obtained if the optical beam is modulating the surface field between low- and high-field conditions. This point is illustrated in Fig. 5, which shows the FK oscillations expected for GaAs if the surface field is modulated between 0 and 5×10^6 V/m. It should be noted that a strongly damped FK line shape has been observed for GaAs at 82 K by Bottka *et al.*[1]

Another interesting result due to Bhattacharya *et al.*[2] is that the ER and PR spectra were somewhat different when the surface field was largest. For instance, for the same applied bias (10 V), the ER line shape showed considerably more damping than was observed for the PR spectrum.

Overall, although there is not a wide variety of published PR data showing clear Franz-Keldysh oscillations, it appears that under the highest-field conditions, Eq. (42) is valid. On the other hand, when the surface field is smaller (but still in the high-field limit) the FK oscillations do not follow the pattern predicted by Eq. (42); in fact, the damped oscillations can only be theoretically obtained if it is assumed that the optical beam is modulating the sample between low- and high-field conditions.

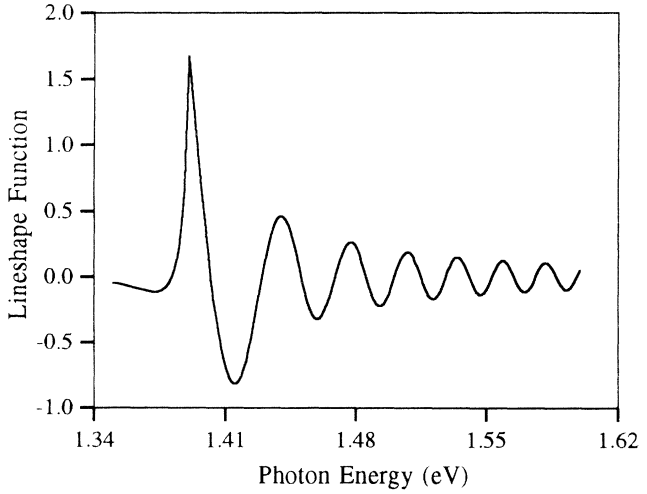

FIG. 5. The high-field, large-modulation PR line-shape function vs the photon energy, in the vicinity of the GaAs direct energy gap (1.39 eV). The surface field is modulated between 0 and 5×10^6 V/m. Using Eq. (29), $\Delta R = R(\xi_{S,0}) - R_0 = \mathrm{Re}[(\alpha - i\beta)\Delta\epsilon(\xi_{S,0})]$.

III. CONCLUSIONS

This work has contributed to the theory of the photoreflectance effect in several ways. First, a general expression for the PR signal was written as a Taylor-series expansion, Eq. (9), in terms of $\Delta\xi_S$, the modulation of the surface electric field. Next, an expression was obtained for $\Delta\xi_S$ in terms of the modulated carrier density, assuming that the field modulation is much smaller than the steady-state electric field. Then, the Fourier-series method was employed in order to rigorously find the harmonic components of the reflectance modulation, for square-wave excitation. Earlier treatments did not employ a full Taylor-series expansion, and did not explicitly consider the time dependence of the exciting beam.[6,8,9]

When the above procedure was followed, the first-order term of the Taylor-series expansion for ΔR yielded a $\ln(\gamma I+1)$ dependence upon the optical excitation intensity I. Since this type of dependence has been widely observed in experiment, it was concluded that higher-order terms in the expansion are not significant under the majority of experimental conditions. Although the PR intensity behavior has previously been linked to the intensity dependence of the surface photovoltage,[8] the present work rigorously shows that the PR signal should indeed have a $\ln(\gamma I+1)$ dependence. A brief review of the literature was carried out in order to identify to what degree the PR intensity dependence has been experimentally determined. It was found that the theoretical logarithmic dependence fits the available data quite well, thus providing a unified theoretical basis for approximate dependences proposed by earlier authors.

Another result of this paper is that the small-modulation PR signal should have a line shape proportional to $\partial R/\partial\xi_S$, due to the apparent domination of the first-order term in the Taylor-series expansion. Therefore, in the high-field limit, the Franz-Keldysh oscillations should be undamped, as shown in Fig. 4. Although the behavior depicted in Fig. 4 has been seen by Bhattacharya *et al.*,[2] they observed a different high-field line shape under zero-bias conditions. In summary, this paper clearly points out that under high-field conditions, the PR line shape is strongly dependent upon the steady-state field in the sample, and upon the degree of field modulation.

Finally, this work suggests that it would be worthwhile to study more deeply the changes in PR line shape obtained when the surface field is increased into the high-field limit. Also, the effects of a steady auxiliary beam upon the PR line shape should be considered, because this auxiliary beam (additional to the modulated excitation beam) is capable of decreasing the magnitude of the surface field without the application of an external bias voltage.

ACKNOWLEDGMENT

The authors gratefully acknowledge the Natural Sciences and Engineering Research Council of Canada (NSERC) for partial support of this research.

APPENDIX A: THE EFFECT OF THE NONUNIFORM ELECTRIC FIELD PERTURBATION UPON THE PHOTOREFLECTANCE LINE SHAPE

Although a full Taylor-series expansion, Eq. (9), was used earlier to determine the PR line shape in the uniform field limit, a simpler relation will be used to explore the effect of the nonuniform electric field upon the PR line shape:

$$\Delta R_{\mathrm{PR}}=\mathrm{Re}\left[\frac{\partial \mathbf{R}}{\partial \epsilon}\frac{\partial \epsilon}{\partial \xi}\Delta\xi\right], \tag{A1}$$

where

$$\mathbf{R}=\left[\frac{1-\epsilon^{1/2}}{1+\epsilon^{1/2}}\right]^2. \tag{A2}$$

Note that Re denotes "the real part of," and that **R** is the complex reflectance. Also, ϵ is the (complex) dielectric constant, which is a function of the probe wavelength, and ξ is the electric field, which is a function of depth into the sample. This approximate relation for ΔR_{PR} neglects the higher-order Taylor-series terms, but its employment allows us to see the effects of the nonuniform field by comparing the results of this appendix with Eq. (28). Also, since the PR effect has been observed experimentally to have a logarithmic intensity dependence, it is very likely that the higher-order terms do not contribute significantly to the PR signal.

Following the work of Aspnes and Frova,[23] when the electric field is nonuniform, Eq. (A1) can be written as

$$\Delta R_{\mathrm{PR}}=\mathrm{Re}\left[\frac{\partial \mathbf{R}}{\partial \epsilon}\left\langle\left[\frac{\partial \epsilon}{\partial \xi}\right]_{\xi_0}\Delta\xi\right\rangle\right], \tag{A3}$$

where

$$\left\langle\left[\frac{\partial \epsilon}{\partial \xi}\right]_{\xi_0}\Delta\xi\right\rangle=-i2K\int_0^{\infty}\exp(i2Kx)\left[\frac{\partial \epsilon}{\partial \xi}\right]_{\xi_0}\Delta\xi(x)dx\ . \tag{A4}$$

In this case, $K=(2\pi/\lambda)(n+ik)$, where λ is the probe wavelength, and n and k are the refractive index and extinction coefficient, respectively, of the sample under equilibrium conditions. Also, x is the distance into the semi-infinite sample. Since $\xi(x)=\xi_S+(\rho/\epsilon_{\mathrm{dc}}\epsilon_0)x$, it is easy to show that except in the narrow range $x=W_0$ to W_1, $\Delta\xi(x)=\Delta\xi_S$, which is independent of x.[10] Therefore,

$$\left\langle\left[\frac{\partial \epsilon}{\partial \xi}\right]_{\xi_0}\Delta\xi\right\rangle=-i2K\Delta\xi_S\int_0^{\infty}\exp(i2Kx)\left[\frac{\partial \epsilon}{\partial \xi}\right]_{\xi_0}dx\ , \tag{A5}$$

where

$$\xi_0(x)=\xi_{S,0}+\frac{\rho}{\epsilon_{\mathrm{dc}}\epsilon_0}x\ . \tag{A6}$$

In order to evaluate Eq. (A5), consider that $\epsilon(\xi)=\epsilon(0)+\Delta\epsilon(\xi)$, where $\Delta\epsilon(\xi)$ is given by Eqs. (37)–(39). Thus, in the high-field limit,

$$\left[\frac{\partial \epsilon}{\partial \xi}\right]_{\xi_0}\propto E^{-2}\left[\tfrac{1}{3}\xi_0^{-2/3}(G+iF)-\tfrac{2}{3}p(E)\xi_0^{-4/3}(G'+iF')\right], \tag{A7}$$

where the functions F and G are evaluated at z_0, and $z_0=p(E)\xi_0^{-2/3}$.

The final relation required to determine ΔR_{PR} is

$$\frac{\partial \mathbf{R}}{\partial \epsilon}=\frac{2(1-\epsilon^{-1/2})}{(1+\epsilon^{1/2})^3}\ . \tag{A8}$$

One problem with evaluating Eq. (A5) is that the derivative term $\partial\epsilon/\partial\xi$ blows up as x increases towards W_0, since it has an ξ_0^{-1}-type dependence, and $\xi_0\to 0$ as $x\to W_0$. In fact, when Eq. (A5) was employed to evaluate the effects of the nonuniform field, the results were not consistent with Fig. 4. It is conceivable that Eq. (A5) can be evaluated as a bounded form by taking its principal value excluding the point $x=W_0$. In that case, the line shape to replace Fig. 4 is expected to be quite different from the one resulting from the assumption of uniform field perturbation. For instance, when Eq. (A5) was evaluated within the range $x=0$ to $x=0.9W_0$, the resulting line shape was similar to that of Fig. 4, except for the presence of a high-frequency modulation envelope, an envelope which is consistent with the decreasing electric field magnitude within the bulk of the sample. It appears that the assumption of uniform field modulation in the SCL [$\Delta\xi(x)=\Delta\xi_s$] is not capable of yielding a bounded result when Eq. (A4) is employed. Overall, the mathematical analysis of the nonhomogeneous line shape is beyond the scope of the present work; furthermore, this kind of predicted behavior is not consistent with the existing experimental data,[1,2] and therefore, it will not be considered further here.

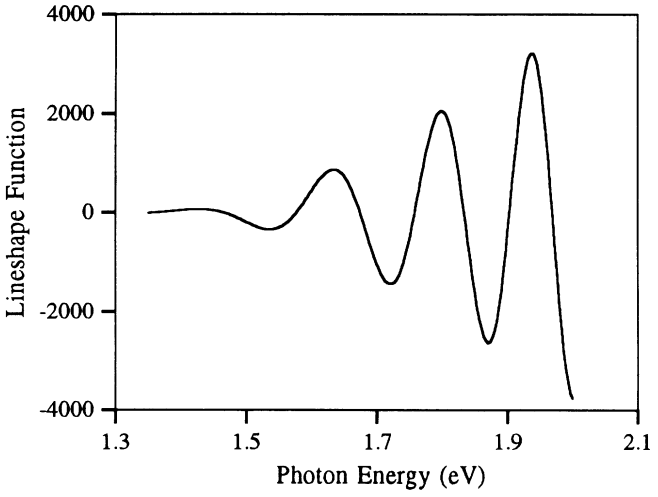

FIG. 6. The high-field, small-modulation, $n=2$, PR lineshape function [Eq. (B2)] vs the photon energy, in the vicinity of the GaAs direct energy gap (1.39 eV). The effective mass is 0.1 times the free electron mass, and $\xi_{S,0}=5\times10^7$ V/m.

APPENDIX B: HIGHER-ORDER ($n > 1$) LINE-SHAPE FUNCTIONS

In this appendix, the $n > 1$ partial derivatives of Eq. (27) will be examined for both the low- and high-field limits. These terms are of importance because they may determine the small-modulation PR line shape when nonlogarithmic intensity dependences are obtained for the PR amplitude.

For the low-field limit, the $n > 1$ partial derivatives are obtained via Eq. (36). In particular, it is easy to show that

$$\frac{\partial^2 R}{\partial \xi_S^2} \propto \frac{R_0}{E^2}\mathrm{Re}\left\{(\alpha - i\beta)\frac{\partial^3}{\partial E^3}[E^2\epsilon(E)]\right\} . \tag{B1}$$

Thus, the $n = 2$ derivative yields the same line shape as the $n = 1$ derivative. Finally, the $n > 2$ derivatives are all zero.

For the high-field limit, the $n > 1$ derivatives are obtained via Eqs. (29) and (42). For example, the $n = 2$ line shape is given by

$$\frac{\partial^2(\Delta\epsilon)}{\partial \xi_S^2} \propto \frac{2}{9}\xi_S^{-5/3}E^{-2}[-(G+iF)+3p\xi_S^{-2/3}(G'+iF') + 2p^2\xi_S^{-4/3}(G''+iF'')] , \tag{B2}$$

where

$$F''(z) = -2\pi\,\mathrm{Ai}(z)\,\mathrm{Ai}'(z) + \tfrac{1}{4}(-z)^{-3/2}u(-z) \tag{B3}$$

and

$$G''(z) = -\pi[\mathrm{Ai}(z)\mathrm{Bi}'(z) + \mathrm{Ai}'(z)\mathrm{Bi}(z)] - \tfrac{1}{4}z^{-3/2}u(z) . \tag{B4}$$

Figure 6 depicts the small-modulation, high-field, $n = 2$ line shape obtained for GaAs using the parameters previously used for Fig.4. The Franz-Keldysh oscillations continue to grow in amplitude as the probe photon energy is increased, a type of behavior which has not been documented in the literature, to the best of our knowledge. In summary, it appears that the PR line shape is not affected by the $n > 1$ terms of Eq. (27).

[1] N. Bottka, D. K. Gaskill, R. S. Sillmon, R. Henry, and R. Glosser, J. Electron. Mater. **17**, 161 (1988).

[2] R. N. Bhattacharya, H. Shen, P. Parayanthal, F. H. Pollak, T. Coutts, and H. Aharoni, Phys. Rev. B **37**, 4044 (1988).

[3] H. Shen, M. Dutta, R. Lux, W. Buchwald, L. Fotiadis, and R. N. Sacks, Appl. Phys. Lett. **59**, 321 (1991).

[4] H. Shen, F. H. Pollak, J. M. Woodall, and R. N. Sacks, J. Electron. Mater. **19**, 283 (1990).

[5] H. Shen, Z. Hang, S. H. Pan, F. H. Pollak, and J. M. Woodall, Appl. Phys. Lett. **52**, 2058 (1988).

[6] W. M. Shen, M. C. A. Fantini, M. Tomkiewicz, and J. P. Gambino, J. Appl. Phys. **66**, 1759 (1989).

[7] E. G. Seebauer, J. Appl. Phys. **66**, 4963 (1989).

[8] T. Kanata, M. Matsunaga, H. Takakura, Y. Hamakawa, and T. Nishino, Proc. SPIE **56**, 1286 (1990).

[9] W. Stossel, K. Colbow, and D. Dunn, Can. J. Phys. **48**, 1675 (1970).

[10] J. L. Shay, Phys. Rev. B **2**, 803 (1970).

[11] R. E. Nahory and J. L. Shay, Phys. Rev. Lett. **21**, 1569 (1968).

[12] I. Broser, R. A. Hoffmann, and H. J. Schulz, Solid State Commun. **8**, 587 (1970).

[13] H. Bauer, C. W. Haberl, U. Ratsch, and W. Stossel, Surf. Sci. **37**, 763 (1973).

[14] D. E. Aspnes, in *Handbook on Semiconductors* edited by M. Balkanski and T. S. Moss (North-Holland, New York, 1980) Vol. 2, Chap. 4A.

[15] B. O. Seraphin, in *Semiconductors and Semimetals,* edited by R. K. Willardson and A. C. Beer (Academic, New York, 1972), Vol. 9, Chap. 1.

[16] D. E. Aspnes and A. Frova, Phys. Rev. B **2**, 1037 (1970).

[17] S. R. Morrison, *Electrochemistry at Semiconductor and Oxidized Metal Electrodes* (Plenum, New York, 1980), p. 68.

[18] D. E. Aspnes, Phys. Rev. **153**, 972 (1967).

[19] H. A. Antosiewicz, in *Handbook of Mathematical Functions,* Natl. Bur. Stand. Appl. Math. Ser. No. 55, edited by M. Abramowitz and I. Stegun (U.S. GPO, Washington, D.C., 1964), p. 446.

[20] D. E. Aspnes and N. Bottka, in *Semiconductors and Semimetals* (Ref. 15), Vol. 9, Chap. 6.

[21] I. Kudman and T. Seidel, J. Appl. Phys. **33**, 771 (1972).

[22] M. Cardona, K. L. Shaklee, and F. H. Pollak, Phys. Rev. **154**, 696 (1967).

[23] D. E. Aspnes and A. Frova, Solid State Commun. **7**, 155 (1968).